Figure 1C

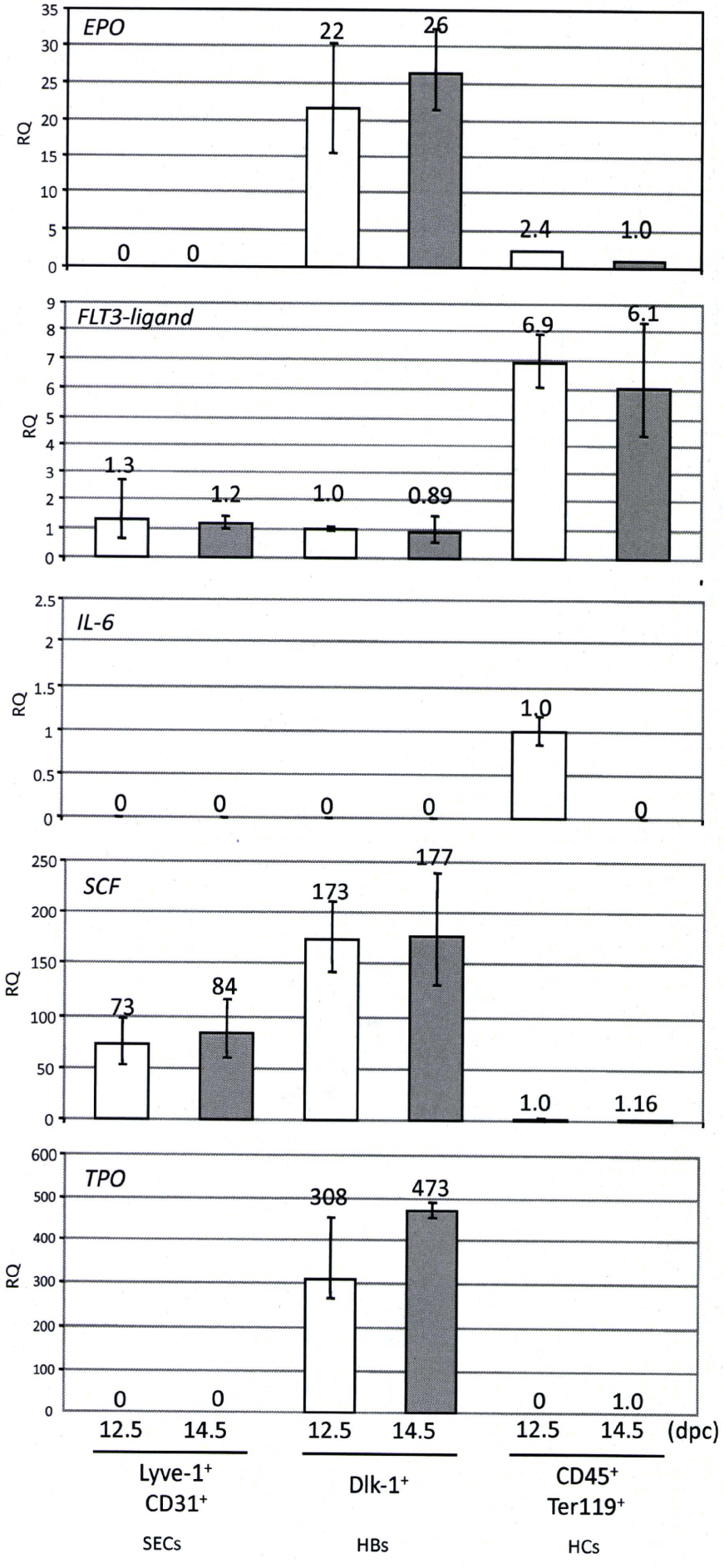
EPO
RQ
0
0
22
26
2.4
1.0
FLT3-ligand
RQ
1.3
1.2
1.0
0.89
6.9
6.1
IL-6
RQ
0
0
0
0
1.0
0
SCF
RQ
73
84
173
177
1.0
1.16
TPO
RQ
0
0
308
473
0
1.0
12.5
14.5
12.5
14.5
12.5
14.5
(dpc)
Lyve-1+ CD31+
SECs
Dlk-1+
HBs
CD45+ Ter119+
HCs

Figure 2A

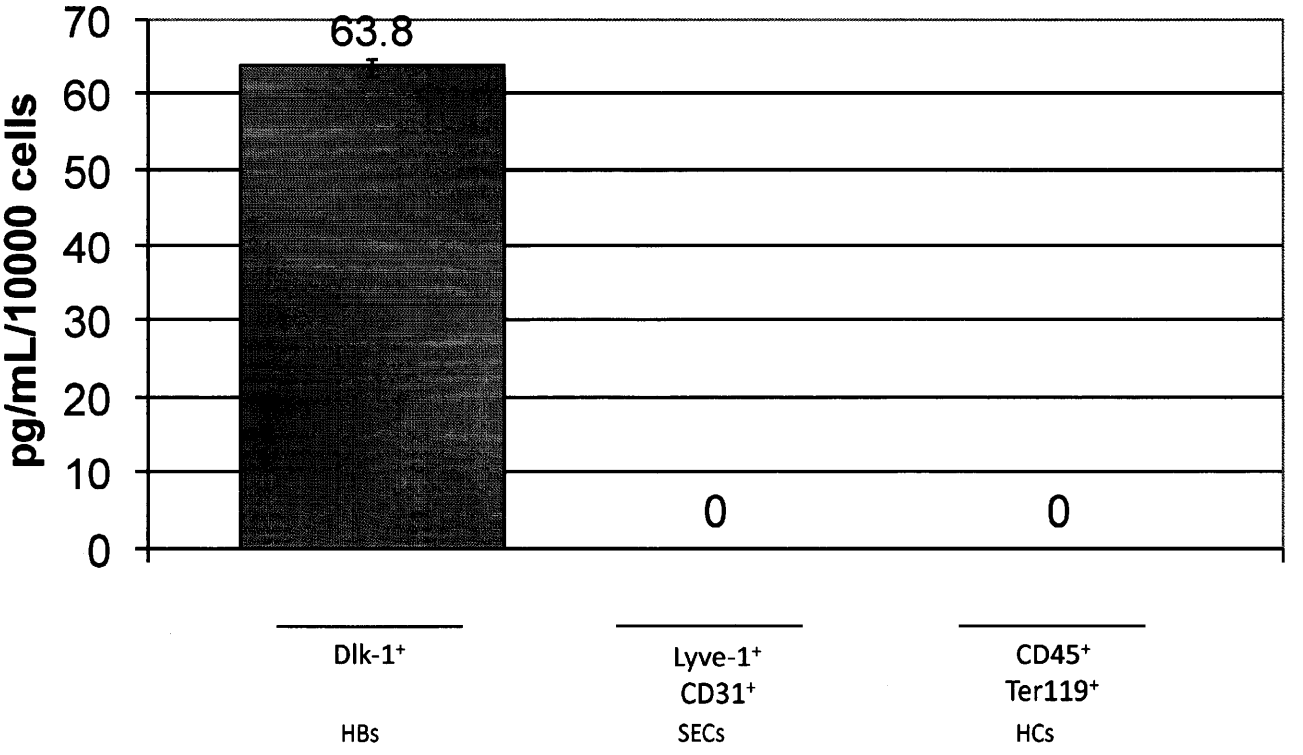

Figure 2B

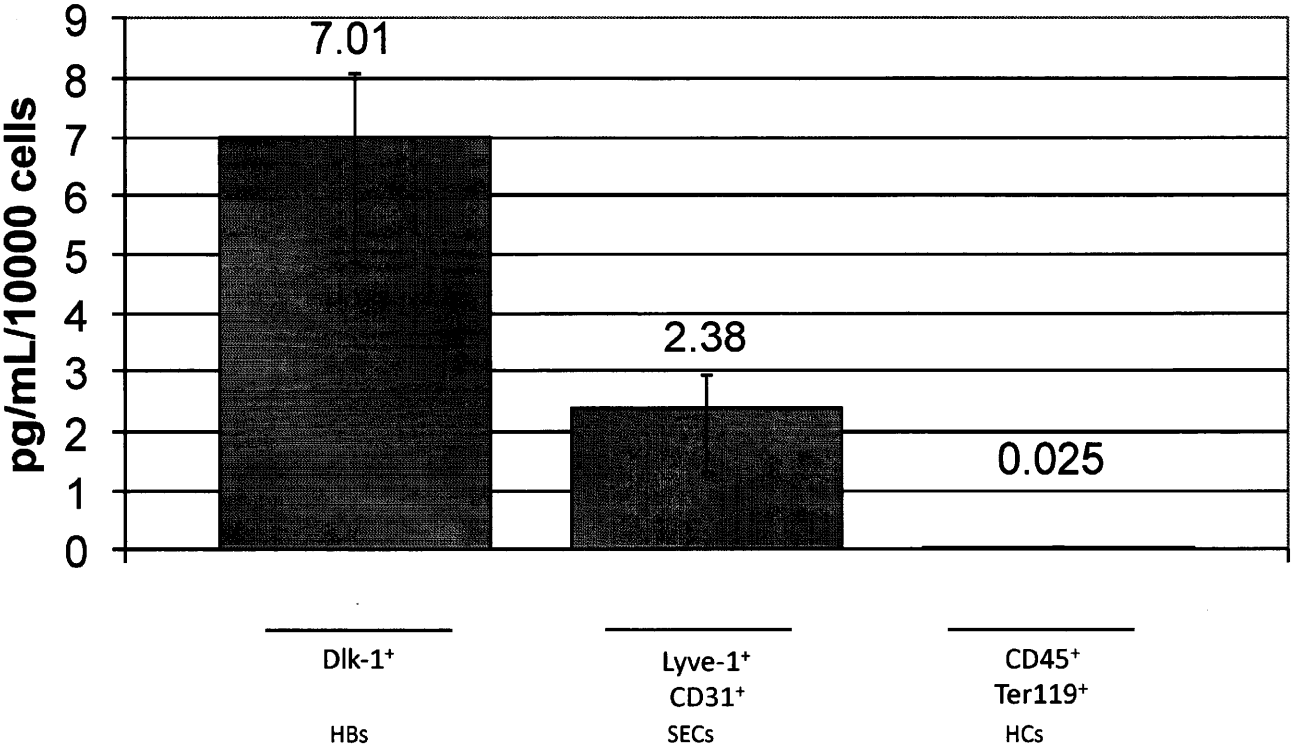

Figure 2C

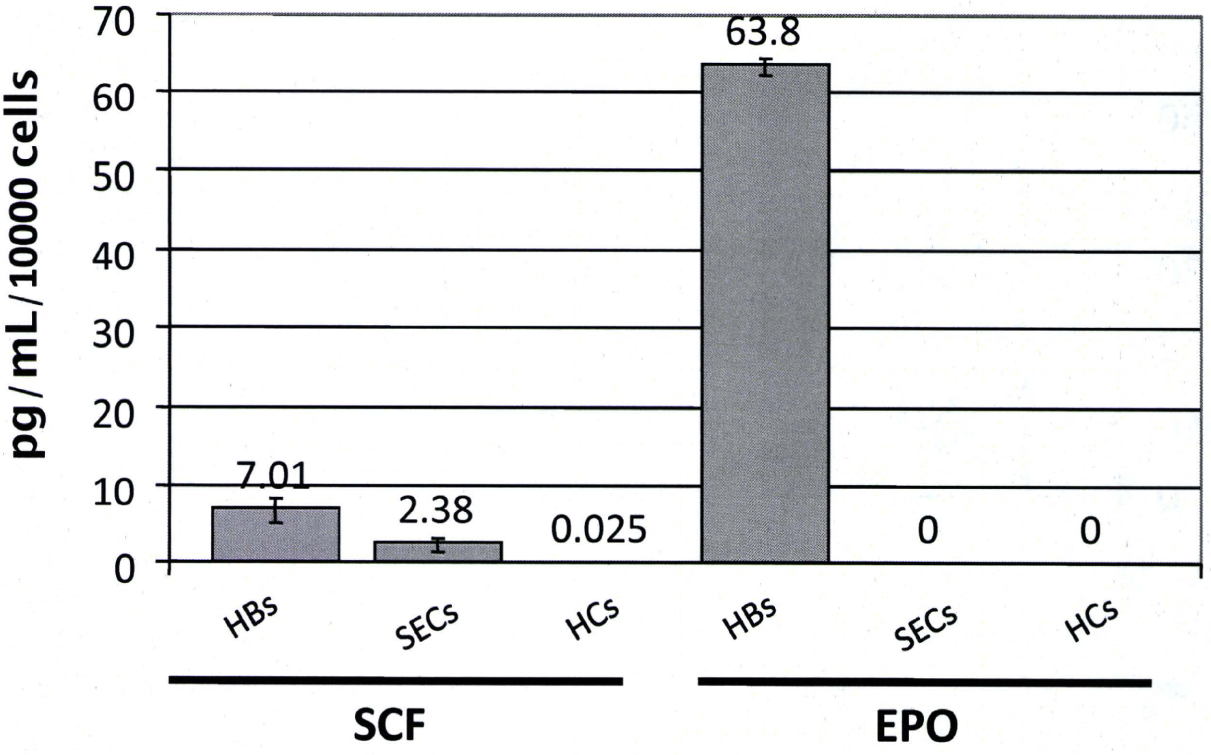

Figure 2D

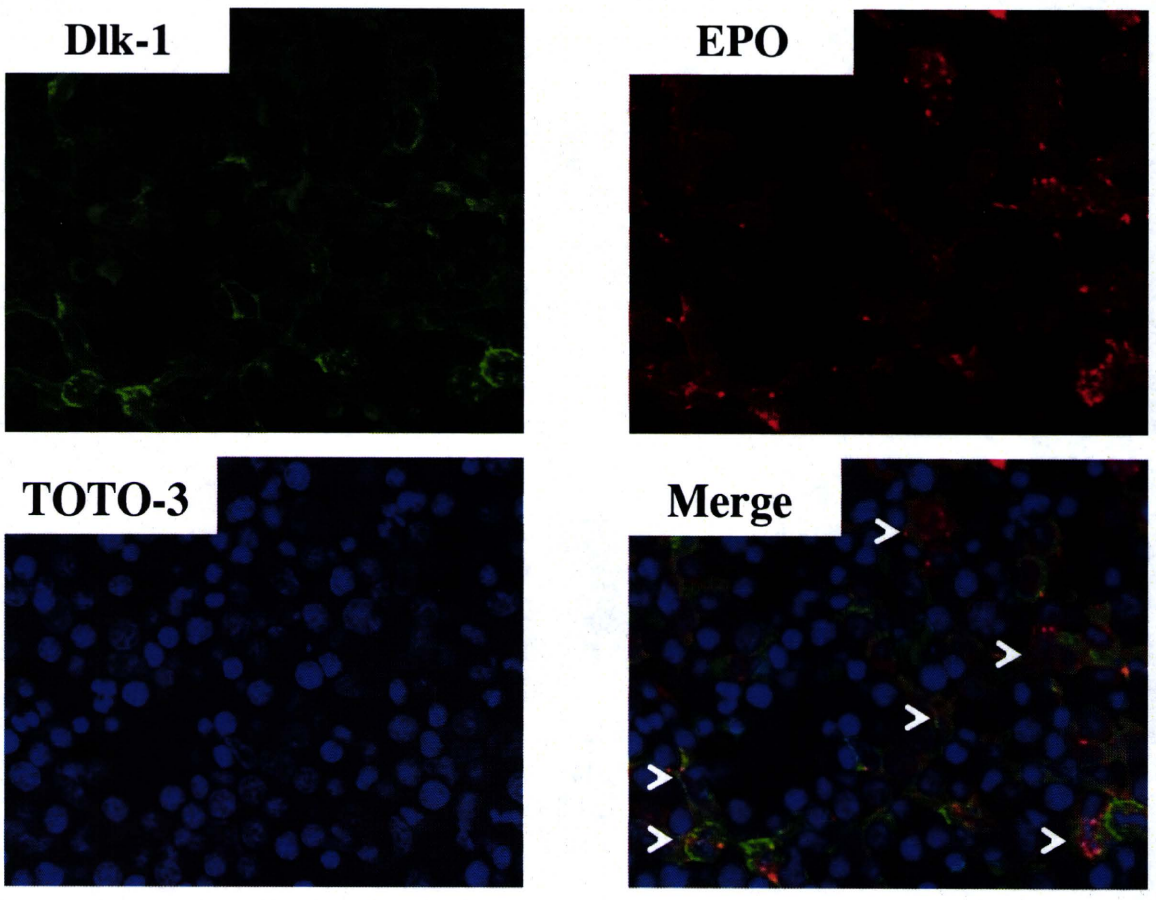

Figure 2E

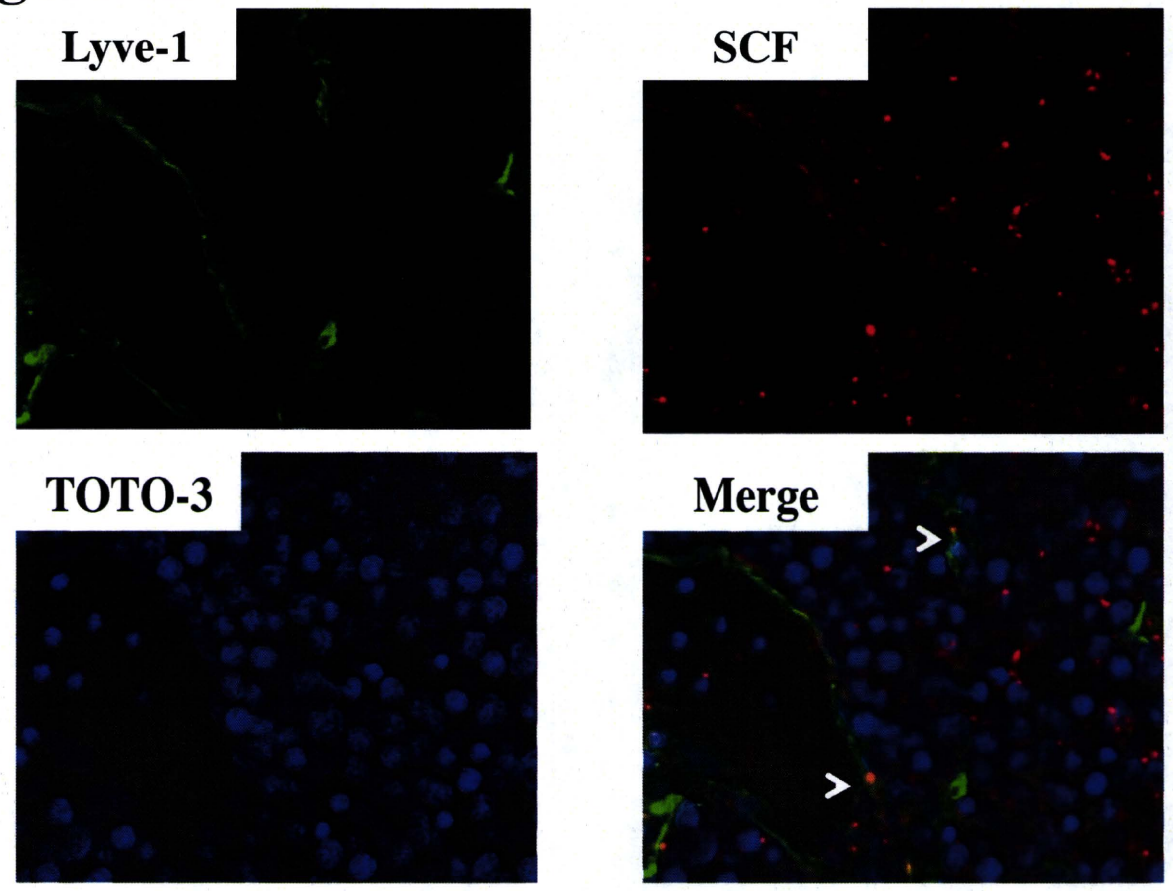

Figure 2F

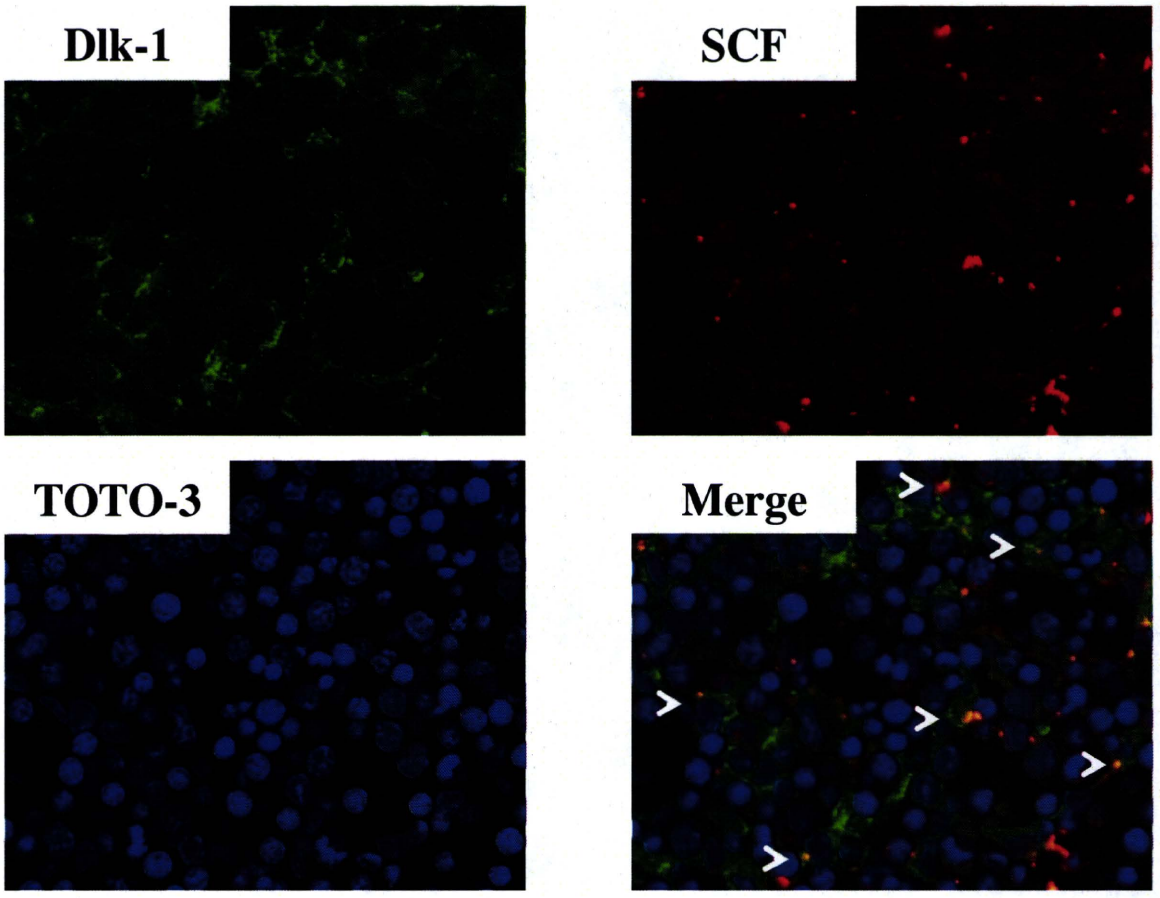

Figure 3A

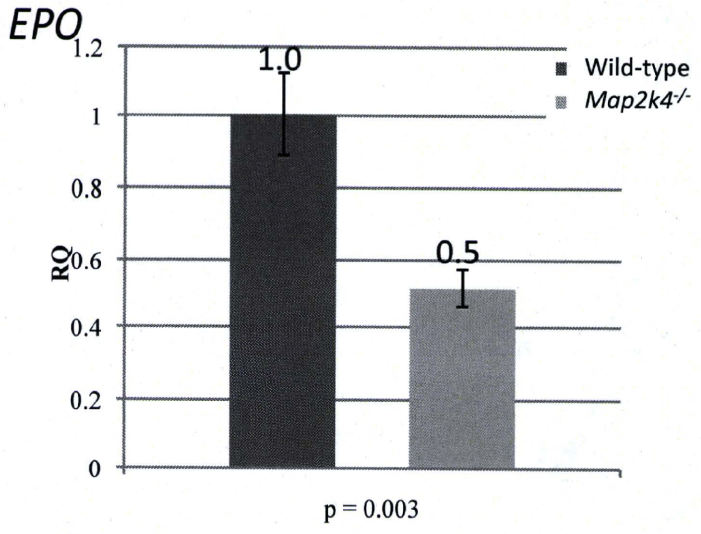
EPO
1.2
1
0.8
0.6
0.4
0.2
0
RQ
1.0
0.5
Wild-type
Map2k4-/-
p = 0.003

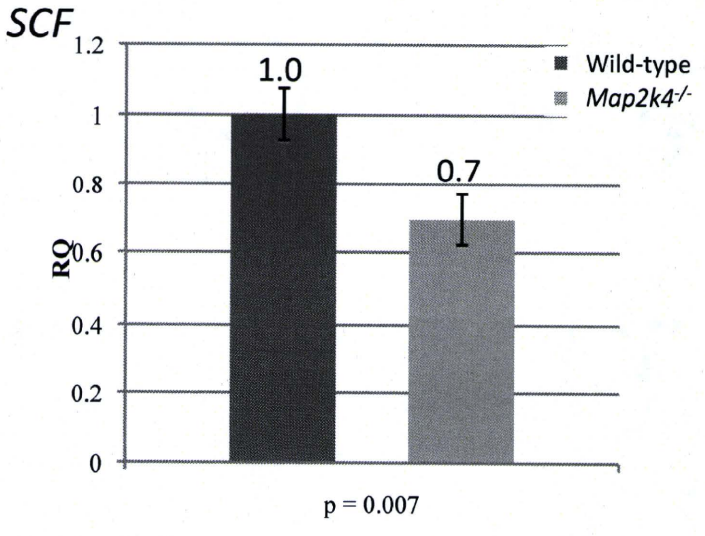
SCF
1.2
1
0.8
0.6
0.4
0.2
0
RQ
1.0
0.7
Wild-type
Map2k4-/-
p = 0.007

Figure 3B

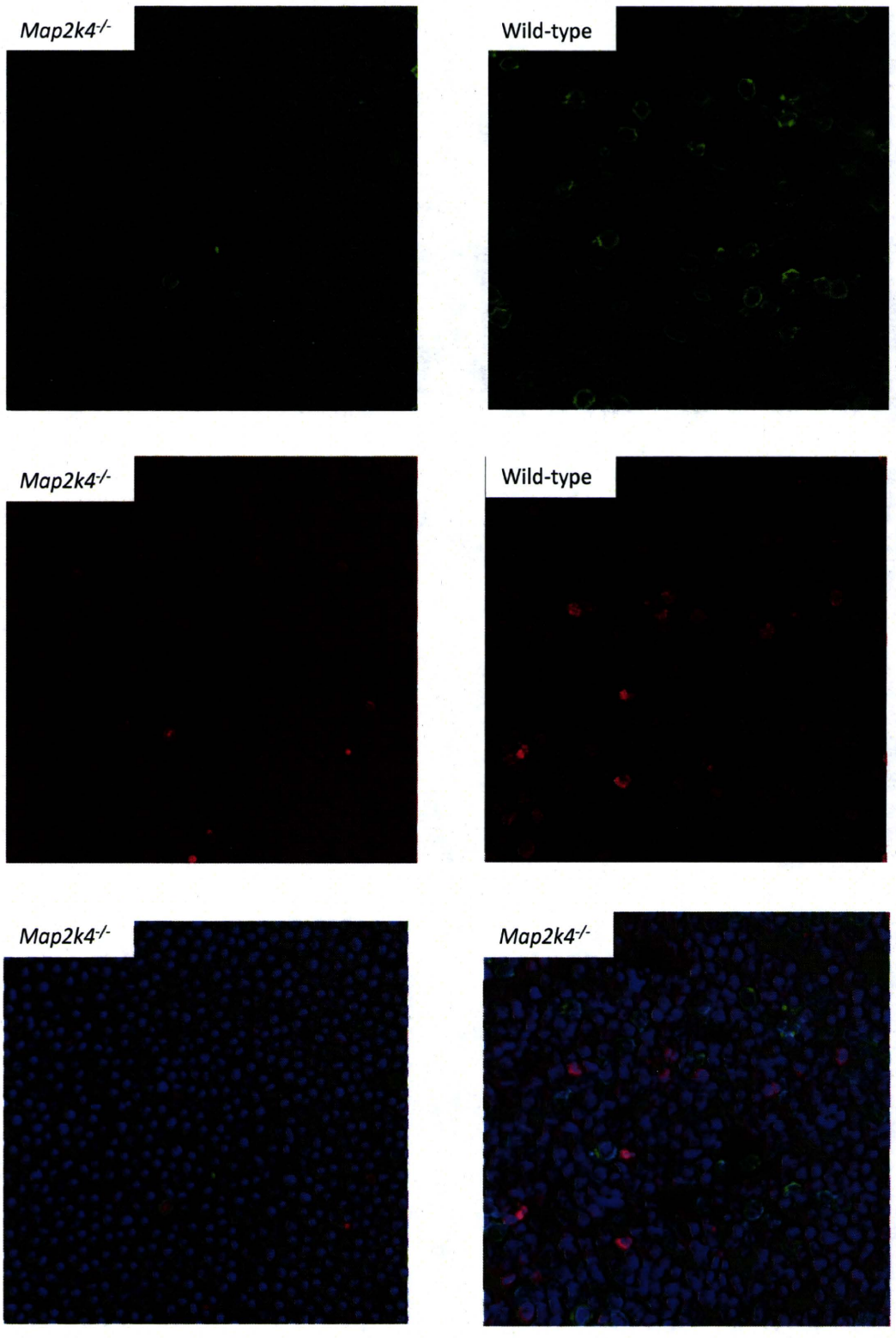

c-Kit Ki-67 TOTO-3

Figure 3C

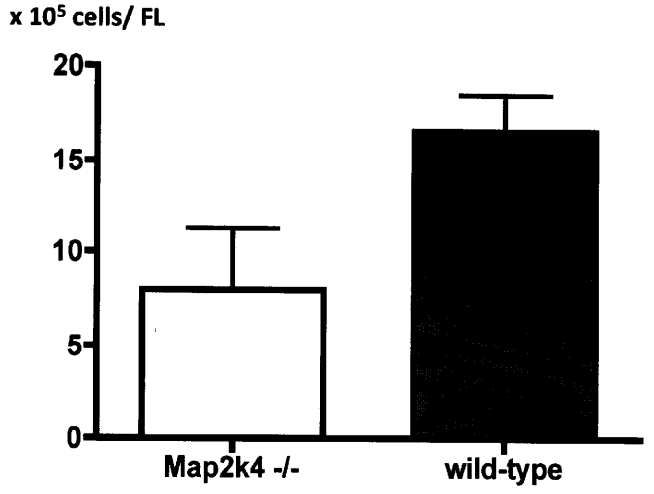

Stem Cell Rev and Rep
DOI 10.1007/s12015-011-9249-3

Variation in Mesodermal and Hematopoietic Potential of Adult Skin-derived Induced Pluripotent Stem Cell Lines in Mice

Tomoko Inoue · Kasem Kulkeaw · Satoko Okayama · Kenzaburo Tani · Daisuke Sugiyama

Abstract Induced pluripotent stem cells (iPSCs) are a promising tool for regenerative medicine. Use of iPSC lines for future hematotherapy will require examination of their hematopoietic potential. Adult skin fibroblast somatic cells constitute a source of iPSCs that can be accessed clinically without ethical issues. Here, we used different methods to compare mesodermal and hematopoietic potential by embryoid body formation of five iPSC lines established from adult mouse tail-tip fibroblasts (TTFs). We observed variation in proliferation and in expression of genes (*Brachyury, Tbx1, Gata1, Klf1, Csf1r*) and proteins (Flk1, Ter119 and CD45) among TTF-derived lines. 256H18 iPSCs showed highest proliferation and most efficient differentiation into mesodermal and hematopoietic cells, while expression levels of the pluripotency genes *Oct3/4, Sox2, Klf4* and *Nanog* were lowest among lines analyzed. By contrast, the 212B2 line, transduced with *c-Myc*, showed lowest proliferation and differentiation potential, although expression levels of *Oct3/4, Sox2* and *Klf4* were highest. Overall, we find that mesodermal and hematopoietic potential varies among iPSCs from an identical tissue source and that *c-Myc* expression likely underlies these differences.

Electronic supplementary material The online version of this article (doi:10.1007/s12015-011-9249-3) contains supplementary material, which is available to authorized users.

T. Inoue · K. Kulkeaw · S. Okayama · D. Sugiyama (✉)
Department of Hematopoietic Stem Cells, SSP Stem Cell Unit,
Kyushu University Faculty of Medical Sciences,
Station for Collaborative Research 1 4F,
3-1-1 Maidashi, Higashi-Ku, Fukuoka 812–8582, Japan
e-mail: ds-mons@yb3.so-net.ne.jp

T. Inoue · K. Tani
Department of Molecular Genetics,
Medical Institute of Bioregulation, Kyushu University,
Fukuoka 812–8582, Japan

Published online: 19 March 2011

Keywords Induced pluripotent stem cells · Tail-tip fibroblasts · Embryoid body · Mesodermal induction · Hematopoietic potential

Introduction

Hematopoietic stem cells (HSCs) are already in use for transplantation therapy for hematological diseases. However, problems associated with HSC transplantation remain, such as a shortage of donors or immunoreactivity caused by HLA mismatching (rejection and graft versus host disease (GVHD)). To overcome these issues, induced pluripotent stem cells (iPSCs) could serve to generate autologous HSCs without the need for a donor. iPSCs have been established from various somatic cells by forced expression of defined factors [1, 2]. These cells display properties similar to embryonic stem cells (ESCs) in terms of differentiation capacity into various cell types, teratoma formation in immuno-deficient mice, and generation of chimeric mice with germ line transmission [3]. Therefore, iPSC technology could enable us to generate cells for clinical purposes without an embryonic source or a donor [4, 5]. Generally, *Oct3/4*, *Sox2*, *Klf4*, and *c-Myc* are retrovirally transduced into somatic cells to initiate reprogramming and establish iPSC lines. Since both expression of the *c-Myc* oncogene and retroviral infection are associated with malignancy, investigators have devised reprogramming protocols lacking *c-Myc* transduction [6] or avoiding use of non-integrated viral vectors [7] or plasmids [8] for gene delivery. Various novel approaches, including combining transcription factors and reporters, have been employed to reprogram various types of somatic cells, such as mouse embryonic fibroblasts (MEFs), adult fibroblasts, pancreatic β-cells, hepatocytes, gastric epithelial cells, B cells, and $CD34^+$ cord blood cells

[9–11]. Among these cell types, adult skin fibroblasts are a desirable potential source of somatic cells, since they can be clinically accessed without ethical problems. To help devise future clinical transplantation therapies, it is necessary to determine which iPSCs derived from tail-tip fibroblasts (TTFs) (adult skin fibroblasts in mice) are most fit to generate HSCs.

Previously, we reported variation in hematopoietic potential among several iPSC lines, regardless of the source of somatic cells [12]. This observation suggested that variation in hematopoietic potential could occur among TTF-derived iPSCs. To address this issue, we analyzed mesodermal and hematopoietic potential in five TTF-derived iPSC lines established using different transcription factors (*Oct3/4, Sox2* and *Klf4* with or without *c-Myc*) or reporter genes (*DsRed* or *GFP*). We demonstrate that both mesodermal and hematopoietic cell number and expression of mesoderm and hematopoietic cell differentiation markers varies among the five lines. Interestingly, 212B2 iPSCs, the only line created via *c-Myc* transduction, exhibited lower capacity to differentiate into mesodermal and hematopoietic cells compared than did the other four iPSCs.

Materials and Methods

iPSCs Maintenance

We used the five lines of tail-tip fibroblast (TTF)-derived iPSCs, such as 256H13, 256H18, 212B2, 212D1 and 335D1, which were kindly provided by Dr. Shinya Yamanaka (Kyoto University). These iPSCs were established by "separate method" as previously described [6]. Briefly, pMX-Oct3/4, pMX-Klf4, pMX-Sox2, and/or pMX-c-Myc plasmids were separately transfected into separate dishes of Plat-E cells using Fugene 6 reagent (Roche Applied Science, Indianapolis, IN). Twenty-four hours after transfection, the medium was replaced with serum-containing DMEM. After 24 h, each virus-containing supernatant was mixed and used for retroviral infection. Concerning iPSCs generation, TTFs were isolated from adult Nanog-GFP-IRES-Puro^r reporter mice or adult DsRed-transgenic mice. For the four-factor transduction, retrovirus-containing supernatants for *Klf4*, *c-Myc*, *Oct3/4*, *Sox2* and *DsRed*, were mixed with the ratio of 1:1:1:1:4. When the fibroblasts were transduced with the three factors, retrovirus-containing supernatants for *Klf4*, *Oct3/4*, *Sox2*, *DsRed* and Mock were mixed with the ratio of 1:1:1:1:4. For transfection, TTFs were seeded at 8.0×10^5 cells in 100-mm dish, without feeder cells. TTFs were incubated in the virus/polybrene-containing supernatants for 24 h. Four days after transduction, TTFs transduced with the three factors were reseeded at 3.5×10^5 cells per 100-mm dish with SNL feeder cells and cultured with ES medium containing DMEM, 15% FBS, 0.1 mM non essential amino acid, 0.1 mM 2-mercaptoethanol (2-ME) and 1000U/ml mouse leukemia inhibitory factor (LIF). TTFs transduced with the four factors were reseeded at 0.5×10^5 cells per 100-mm dish with feeder cells. Thirty to forty days after transduction, the colonies were selected for expansion. Drug selection with puromycin (1.5 μg/ml) was done for 212B2, 212D1 and 335D1 iPSCs. 256H13 and 256H18 iPSC lines were established without drug selection [6]. Twenty to thirty percent efficiency was achieved in transfection of all five iPSC lines.

We firstly expanded these iPSC lines with mitomycin-C (MMC)-treated mouse embryonic fibroblasts (MEFs) in StemMedium (DS Pharma Biomedical, Hyogo, Japan) containing 0.1 mM 2-ME (Nacalai Tesque, Inc., Kyoto, Japan) and 1000 U/ml mouse LIF (prepared in Dr. Minetaro Ogawa's Laboratory). The passage number (P) for each line used in this study was as follows; 256H13 (P.6-P.9), 256H18 (P.8-P.10), 212B2 (P.9), 212D1 (P.6), and 335D1 (P.8-P.10).

Fig. 1 Comparison of five iPSC lines during EB culture. **a** TTF-derived iPSCs. Morphology of five iPSC lines maintained on mitomycin-C (MMC)-treated mouse embryonic fibroblasts (MEFs) is shown by phase contrast and DsRed or GFP fluorescence. 256H13 and 256H18 iPSCs constitutively express DsRed under control of the *β-actin* (*Actb*) promoter, while 212B2, 212D1 and 335D1 iPSCs express GFP under control of the *Nanog* promoter. Scale bars are 200 μm. **b** Cell morphology during iPSC differentiation. Differentiation of iPSCs at days 4, 5, and 6. Phase contrast images. Scale bars are 100 μm. **c** Total number of viable cells from each of five lines during the course of EB formation. Four, five and six days after EB formation, differentiated-iPSCs were collected and viable cells counted using Trypan blue dye

Embryoid Body (EB) Formation

Before EB formation, iPSCs were separated from feeder cells by 0.5-hour incubation to eliminate the attached MEF cells. Then, iPSCs expressing stage-specific embryonic antigen-1 (SSEA-1) were purified by magnetic cell separation (MACS, Miltenyi Biotec, Auburn, CA). iPSCs (6×10^4 cells) were cultured in 3 ml of EB medium, which contains Iscove's Modified Dulbecco's Medium (IMDM, SIGMA-ALDRICH, St. Louis, MO) containing 15% FBS (a pre-selected batch showing the highest efficiency in inducing hematopoietic cells), 2 mM L-glutamine (SIGMA-ALDRICH), 0.0026% (vol/vol) monothioglycerol (MTG; Wako Pure Chemical Industries, Osaka, Japan), 50 μg/ml L-ascorbic acid (Wako Pure Chemical Industries), 10 U/ml penicillin, and 10 μg/ml streptomycin (SIGMA-ALDRICH).

For mesodermal cell differentiation, no cytokine was added in the EB medium. Petri dishes (60-mm in diameter, Kord-Valmark™, Ontario, Canada) were used to generate EBs. On culture days 4, 5, and 6, cells were collected by gentle pipetting, washed once in PBS, and then incubated in

a

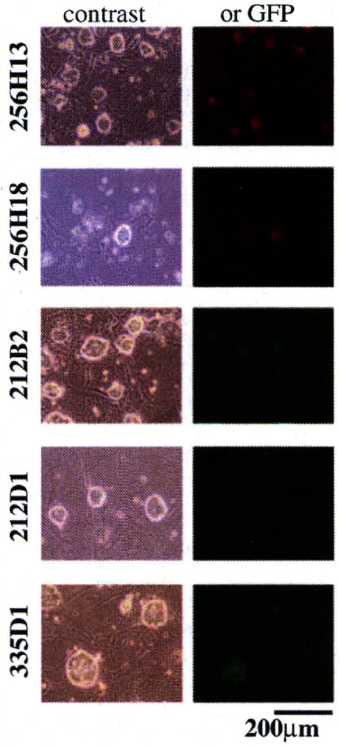

iPSC line	Transduced genes	Reporter gene	Transduction method	Viral vector	Genetic selection
iPS-TTF-FB/DsRed-256H13	Oct3/4, Klf4, Sox2	Actb-DsRed	Retrovirus	pMX-Oct3/4 pMX-Klf4 pMx-Sox2	w/o
iPS-TTF-FB/DsRed-256H18	Oct3/4, Klf4, Sox2	Actb-DsRed	Retrovirus	pMX-Oct3/4 pMX-Klf4 pMX-Sox2	w/o
iPS-TTF-FB/Ng-212B2	Oct3/4, Klf4, Sox2, c-Myc	Nanog-GFP	Retrovirus	pMX-Oct3/4 pMX-Klf4 pMX-Sox2 pMX-c-Myc	Nanog
iPS-TTF-FB/Ng-212D1	Oct3/4, Klf4, Sox2	Nanog-GFP	Retrovirus	pMX-Oct3/4 pMX-Klf4 pMX-Sox2	Nanog
iPS-TTF-FB/Ng-335D1	Oct3/4, Klf4, Sox2	Nanog-GFP	Retrovirus	pMX-Oct3/4 pMX-Klf4 pMX-Sox2	Nanog

b

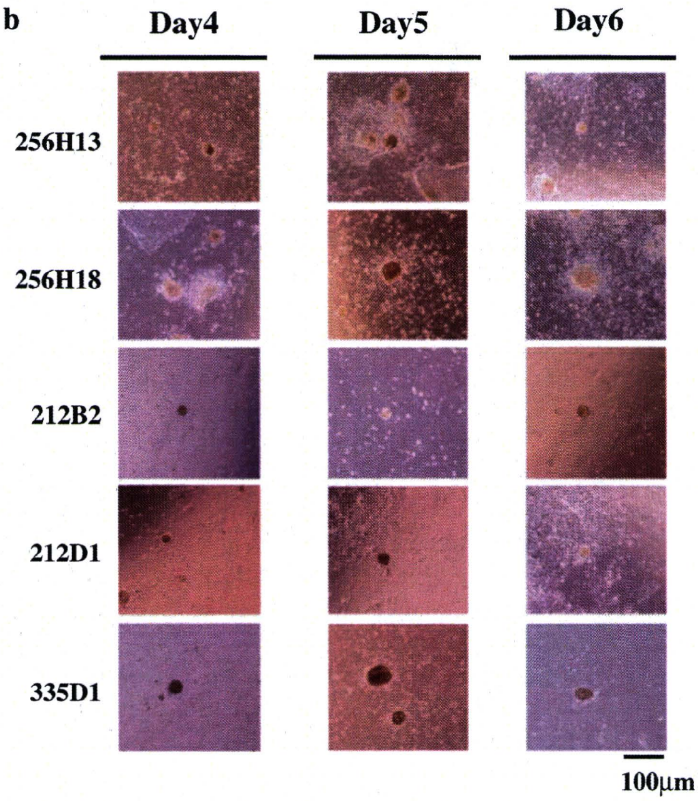

c

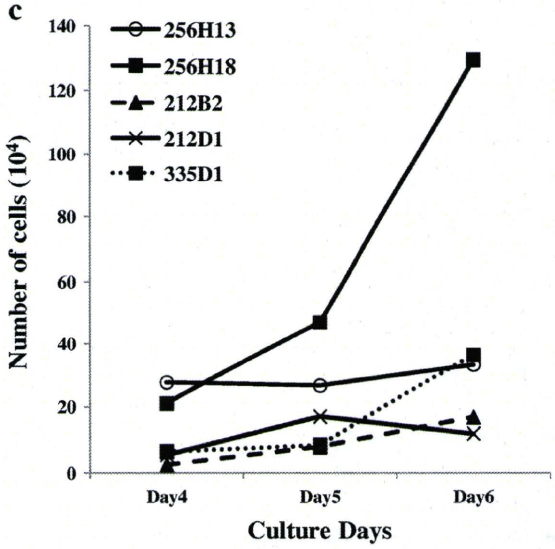

Cell Dissociation Buffer (Life Technologies, Carlsbad, CA) at 37°C for 30 min. An equal volume of medium containing 10% FBS was added and mixed gently by pipetting, and the cell suspension was passed through a 40-μm nylon mesh. The number of living cells was determined by staining with 0.4% Trypan blue (Life Technologies). For hematopoietic cell differentiation, SCF (stem cell factor), IL (interleukin)-3, EPO (erythropoietin), IL-6 and G-CSF (granulocyte colony-stimulating factor) were added in the EB medium. Petri dishes were used to generate EBs. On culture days 9, cells were collected and counted as mentioned above.

Flow Cytometry

To analyze mesodermal cells from iPSCs, cells cultured for 4, 5, and 6 days were collected as mentioned in 'EB formation' and stained with an APC-conjugated anti-CD324 (E-cadherin) antibody (Ab) (Alexa Fluor®647, eBioscience, San Diego, CA), a Pacific Blue™ -conjugated anti-mouse Flk1 (VEGFR2) Ab (BioLegend, San Diego, CA), a biotin-conjugated anti-mouse CD140α (PDGFRα) Ab (eBioscience) and an APC-Cy7-conjugated streptavidin (BD Biosciences, San Jose, CA). Biotin-conjugated antibody was used as a primary antibody and fluorescence-conjugated streptavidin was used as a secondary reagent, respectively. E-cadherin$^-$/Flk1$^+$ cells were defined as lateral mesodermal cells and E-cadherin$^-$/PDGFRα$^+$ cells as paraxial mesodermal cells, respectively.

To analyze hematopoietic cells from iPSCs, cells cultured for 9 days were collected as mentioned in 'EB formation' section and stained with an APC-Cy7-conjugated anti-mouse Ter119 Ab (eBioscience), a PB-conjugated anti-mouse CD45 Ab (BioLegend), an APC-conjugated anti-mouse F4/80 (BioLegend), a biotin-conjugated anti-mouse Gr-1 Ab (eBioscience) and PE-Cy7-conjugated streptavidin (BD Biosciences). For Mac1 Ab, a PE-conjugated anti-mouse Mac1 Ab (BioLegend) was used for GFP-expressing iPSCs (212B2, 212D1, and 335D1). And a biotin-conjugated anti-mouse Mac1 Ab (eBioscience) and a PE-Cy7-conjugated streptavidin were used for DsRed-expressing iPSCs, respectively. Biotin-conjugated antibody was used as a primary antibody and fluorescence-conjugated streptavidin was used as a secondary reagent, respectively. Ter119 positive cells were defined as erythroid cells, CD45 positive cell as leukocytes, Mac1$^+$/F4/80$^+$ cells as macrophages and Gr-1$^+$/F4/80$^-$ cells as granulocytes, respectively.

To stain dead cells, propidium iodide (PI, Life Technologies, Eugene, Oregon) was used for GFP-expressing iPSCs, and TO-PRO®-1 iodide (Life Technologies) was used for DsRed-expressing iPSCs. Cells were analyzed using a FACS Aria cell sorter (Becton Dickinson, Franklin Lakes, NJ). Data files were analyzed using FlowJo software (Tree Star, San Carlos, CA).

Fig. 2 Mesodermal cell differentiation from iPSCs. **a** Flow cytometric analysis of mesodermal cells from all five iPSC lines at days 4, 5, and 6 during the course of EB culture. Lateral mesodermal cells were evaluated based on lack of expression of the surface marker E-cadherin (CD324, epithelial cadherin) and expression of Flk1 (CD309, VEGFR2) (*upper panel*). Paraxial mesodermal cells were evaluated based on lack of expression of E-cadherin and expression of PDGFRα (*lower panel*). **b** Quantitative real-time PCR analysis was used to detect the mesodermal markers *Flk1*, *Tbx6* and *Brachyury* at day 4 of EB culture. Data was normalized to *β-actin* expression

Quantitative Real-Time PCR

Total RNA was isolated with the RNAqueous-Micro Kit (Ambion, Austin, TX). A high-capacity cDNA Archive kit (Applied Biosystems, Foster City, CA) was used to synthesize cDNA from mRNA. mRNA levels were normalized to *β-actin* as an internal control. In real-time PCR, mRNA levels were analyzed by the SYBR Green method with gene-specific primers or Taqman probe methods. Genes analyzed by SYBR Green included *Oct3/4* (Fw; gcagctcagccttaagaacatgt, Rv; cgatttgcatatctcctgaaggt), *Klf4* (Fw; gaactcacacaggcgagaaacc, Rv; tcggagcgggcgaatt), *Sox2* (Fw; atcaggctgccgagaatcc, Rv; ctcaaactgtgcataatggagt taaaaa) and *Nanog* (Fw; caaaaccaaaggatgaagtgcaa, Rv; gtgctgagcccttctgaatca). *Oct3/4*, *Klf4*, and *Sox2* primer sets recognized both internal and external sequences. Mouse *β-actin* (Fw; gctctggctcctagcaccat, Rv; gccaccgatccacacagagt) served as an internal control. Genes analyzed using the Taqman probe (Applied Biosystems) included *Flk1* (Mm01222421_m1), *Brachyury* (Mm01318252_m1), *Tbx6* (Mm00441681_m1), *Gata1* (Mm01352636_m1), *Klf1* (Mm00516096_m1), *CD45* (Mm01293577_m1), *Csf1r* (Mm01266652_m1), *PU.1* (Mm00488142_m1), and *c-Myc* (Mm00487804_m1). Mouse *β-actin* (4352933E) served as an internal control.

Results

Morphology and EB Formation Capacity of TTF-derived iPSCs

In this study, we cultured 5 induced pluripotent stem cell (iPSC) lines—256H13, 256H18, 212B2, 212D1, and 335D1—which were established by different protocols from adult mouse tail-tip fibroblasts (TTF) [6]. The *DsRed* gene is downstream of the *β-actin* (*ACTB*) gene in 256H13 and 256H18 iPSCs, whereas *GFP* is downstream of *Nanog* and serves an indicator of pluripotency in 212B2, 212D1, and 335D1 iPSCs, as summarized in Fig. 1a. *Oct3/4*, *Klf4*, *and Sox2* genes were transduced into TTFs to establish all iPSC lines, while the 212B2 line was also transduced with *c-Myc*. All iPSC colonies exhibited round morphology and exhibited large nucleoli and low cytoplasmic content.

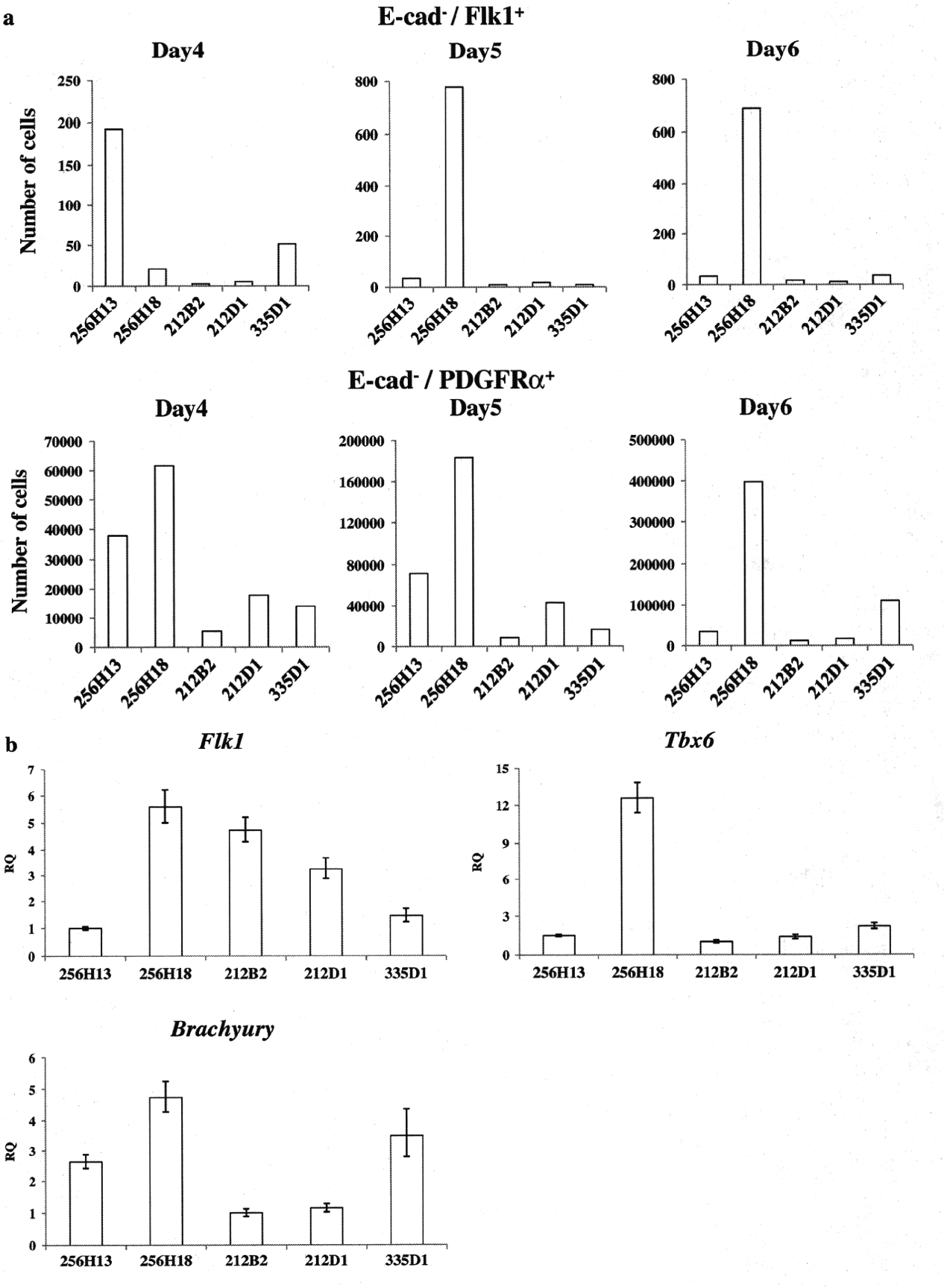
a
E-cad- / Flk1+
Day4
Day5
Day6
Number of cells
250
200
150
100
50
0
800
600
400
200
0
256H13
256H18
212B2
212D1
335D1
E-cad- / PDGFRα+
Day4
Day5
Day6
Number of cells
70000
60000
50000
40000
30000
20000
10000
0
200000
160000
120000
80000
40000
500000
400000
300000
200000
100000
b
Flk1
Tbx6
Brachyury
RQ
7
6
5
4
3
2
1
0
15
12
9
6
3

335D1 formed larger colonies than other lines (Fig. 1a). 212B2, 212D1and 335D1 lines were GFP-positive, indicative of *Nanog* expression and pluripotency.

Next, we performed differentiation culture using the method of embryoid body (EB) formation without cytokines (Supplementary Fig. 1a). Four, five and six days after EB formation, we observed the cultured cells microscopically (Fig. 1b) and evaluated proliferation by cell counting (Fig. 1c). All iPSCs formed EBs, although EB size and the number of adherent cells varied among lines (Fig. 1b). 212B2 and 335D1 iPSCs formed round EBs, although 335D1-derived EBs were larger than 212B2-derived EBs. By contrast, cultured 256H13, 256H18 and 212D1 iPSCs gave rise to adherent cells as well as round EBs. 256H18-derived EBs were larger than those derived from 212D1 cells at day 5 and, in the case of 256H18, adherent cells were observed most frequently (Fig. 1b). In terms of proliferation, the number of 256H13-derived cells increased at day 4 (2.75×10^5 cells) and then plateaued. The number of 256H18 iPSCs also increased gradually through the culture period and then plateaued. 256H18 iPSCs-derived cells gradually increased during the culture and plateaued at day 5 (4.70×10^5 cells). Although 212B2 and 335D1 lines increased gradually during the culture period, their viable cell number at day 6 (1.69×10^5 and 3.63×10^5, respectively) was lower than that of 256H18 iPSCs. By contrast, the number of 212D2-derived cells increased from day 4 (5.50×10^4 cells) to 5 (1.70×10^5 cells), and then decreased (1.19×10^5 cells). There was no significant difference among all iPSC lines in cell viability during EB culture (Supplementary Fig. 2). Taken together, our results indicate that EB formation and cell proliferation varies among five iPSC lines derived from the same tissue.

Mesodermal Potential of TTF-derived iPSCs

To assess iPSC hematopoietic potential, we first examined their mesodermal potential, as hematopoietic cells are mesodermal in origin [13, 14]. ESC mesodermal differentiation was monitored using three markers: lack of E-cadherin (a marker of both ectoderm and endoderm in early mouse development [15]) expression, expression of platelet-derived growth factor receptor α (PDGFRα) and Flk1 (also known as VEGF receptor 2) [16, 17]. We compared the number of iPSC-derived E-cadherin$^-$/Flk1$^+$ cells, representing lateral mesoderm, and E-cadherin$^-$/PDGFRα$^+$ cells, representing paraxial mesoderm, at days 4, 5 and 6 of EB culture, since ESC-derived EBs [18, 19] contain Flk1$^+$ mesodermal cells at 4 to 4.5 days of culture and iPSC-derived EBs contain Flk1$^+$ cells at 5 days of culture [12]. The emergence of E-cadherin$^-$/Flk1$^+$ cells from the 256H13 line was the most rapid among the five lines tested, and the number of cells in this fraction was highest at day 4 (193 cells) and then decreased (Fig. 2a, upper panel). The number of E-cadherin$^-$/Flk1$^+$ cells from 256H18 was the highest among the five lines tested (day 5; 776 cells) (Fig. 2a, upper panel). In contrast, the number of 212B2 and 212D1 iPSC-derived E-cadherin$^-$/Flk1$^+$ cells was lower than that seen in the other three lines. The number of E-cadherin$^-$/PDGFRα$^+$ cells from 256H18 was highest among the five lines (day 6; 3.97×10^5 cells) (Fig. 2a, lower panel). The number of E-cadherin$^-$/PDGFRα$^+$ cells from 256H13 and 212D1 lines increased from days 4 to 5 and then decreased, whereas those from 256H18 and 212B2 lines gradually increased from days 4 to 6. The number of E-cadherin$^-$/PDGFRα$^+$ cells from 335D1 dramatically increased from day 5 (1.59×10^4 cells) to day 6 (1.10×10^5 cells) (Fig. 2a, lower panel). To confirm iPSC mesodermal cell differentiation, we employed PCR to examine expression of the mesoderm markers *Flk1* (lateral mesoderm), *Tbx6* [20] (paraxial mesoderm) and *Brachyury* [21] (pan-mesodermal marker). *Flk1* expression was lowest in 256H13-derived cells at day 4 of culture (Fig. 2b), whereas it was highest in 256H18-derived cells over days 4 to 6 (Supplementary Fig. 3 and 5). *Tbx6* expression at day 4 was highest in 256H18-derived iPSCs, whereas *Tbx6* expression was highest at days 5 and 6 in 335D1- and 256H13-derived cells, respectively (Fig. 2b and Supplementary Fig. 3 and 5). *Brachyury* expression at day 4 was higher in 256H18- and 335D1-derived cells compared to others (Fig. 2b), whereas it was highest at days 5 and 6 in 335D1- and 256H13-derived cells, similar to *Tbx6* expression (Supplementary Fig. 3 and 5). There was a trend in mesodermal differentiation. Early differentiation in 256H13 cells was observed, whereas late differentiation in 335D1 (Fig. 2a). 256H18 cells differentiated into both lateral and paraxial mesoderm most frequently. Overall differences we observed in mesodermal differentiation potential suggest variation in mesodermal potential of adult skin-derived induced pluripotent stem cell lines in mice.

Fig. 3 Hematopoietic cell differentiation from iPSCs. **a** Differentiated iPSCs were collected at day 9 of EB culture and Ter119$^+$ erythroid cells were evaluated by flow cytometry. **b** Quantitative real-time PCR analysis was used to detect expression of the erythroid genes *Gata1* and *Klf1* at day 9 of EB culture. Data was normalized to *β-actin* expression. **c**, **d** Differentiated iPSCs were collected at day 9 of EB culture and evaluated by flow cytometry for (**c**) CD45$^+$ leukocytes and (**d**) myeloid cells (Mac1$^+$/F4/80$^+$ macrophages and Gr-1$^+$/F4/80$^-$ granulocytes). **e** Quantitative real-time PCR analysis was used to detect expression of the myeloid-related genes *CD45*, *Csf1r* and *PU.1* at day 9 of EB culture. Data was normalized to *β-actin* expression

Hematopoietic Potential of TTF-derived iPSCs

Next we examined cell number and the percentage of erythroid and myeloid cells emerging during EB formation at day 9 of culture in the presence of cytokines (Supplementary Fig. 1b). Flow cytometry analysis showed that

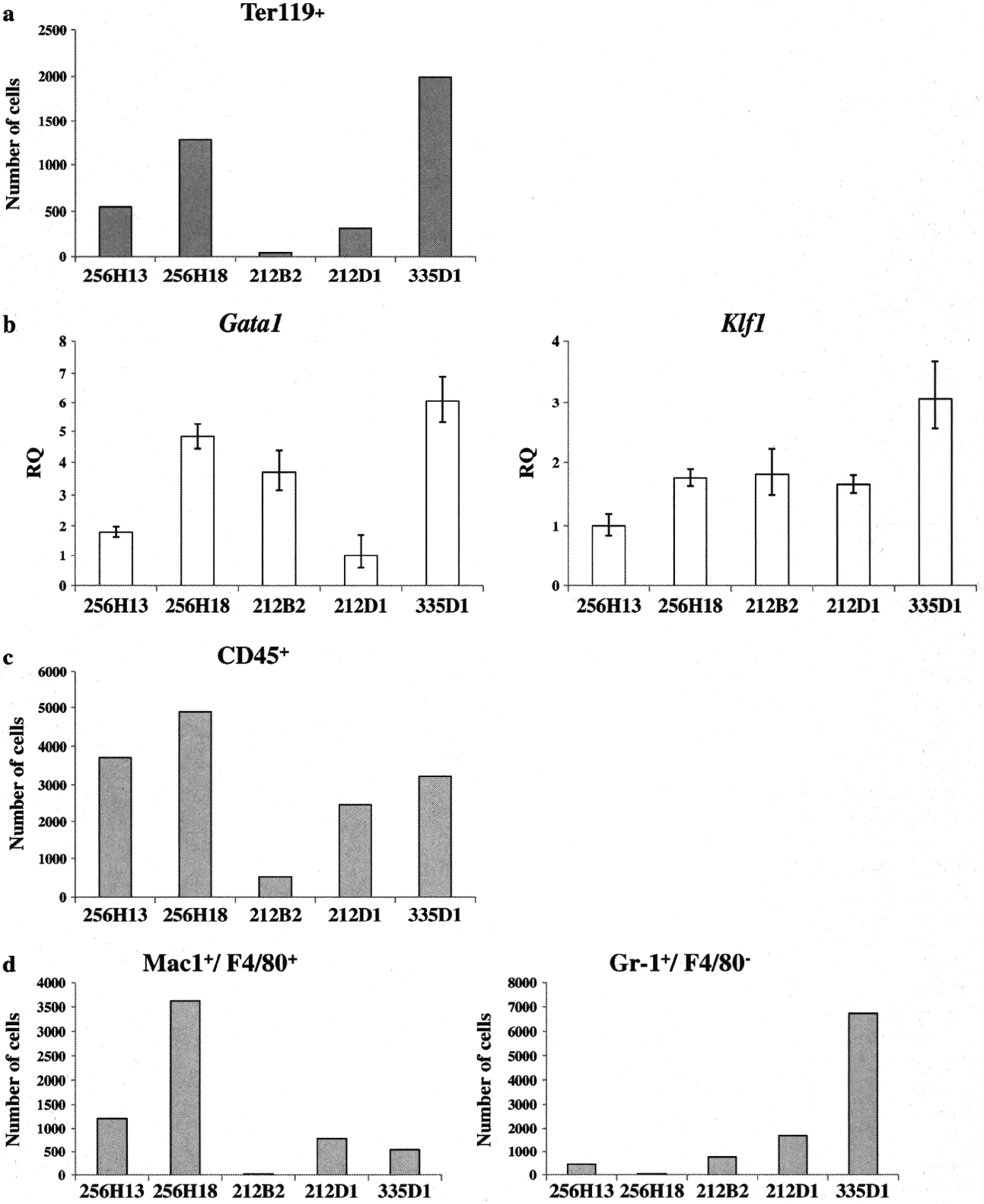
a
Ter119+
Number of cells
2500
2000
1500
1000
500
0
256H13
256H18
212B2
212D1
335D1
b
Gata1
RQ
8
7
6
5
4
3
2
1
0
256H13
256H18
212B2
212D1
335D1
Klf1
RQ
4
3
2
1
0
256H13
256H18
212B2
212D1
335D1
c
CD45+
Number of cells
6000
5000
4000
3000
2000
1000
0
256H13
256H18
212B2
212D1
335D1
d
Mac1+/ F4/80+
Number of cells
4000
3500
3000
2500
2000
1500
1000
500
0
256H13
256H18
212B2
212D1
335D1
Gr-1+/ F4/80-
Number of cells
8000
7000
6000
5000
4000
3000
2000
1000
0
256H13
256H18
212B2
212D1
335D1

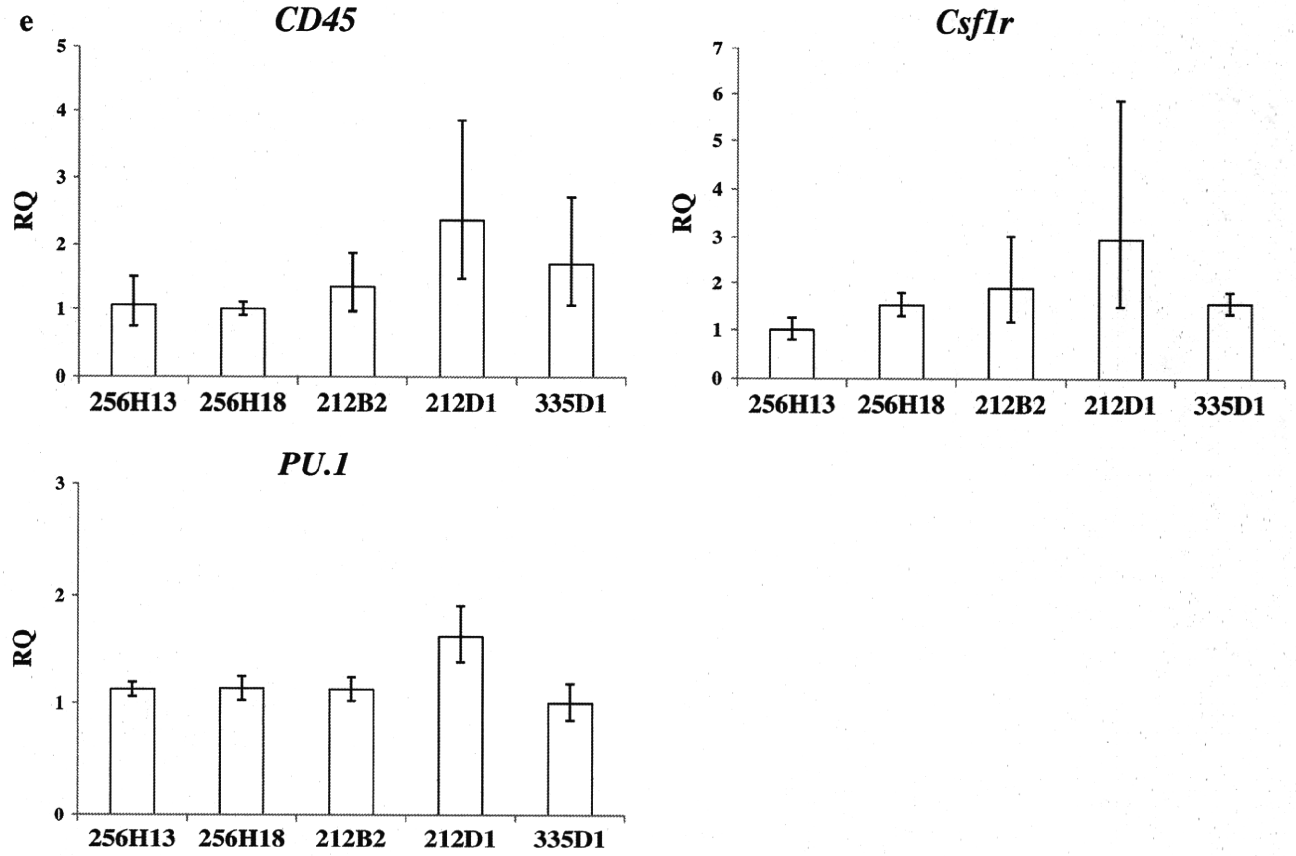

Fig. 3 (continued)

lines 256H18 and 335D1 efficiently differentiated into Ter119$^+$ erythroid cells at 0.35% (1280 cells) and 0.72% (1991 cells), respectively. By contrast, 212B2 cells differentiated into Ter119$^+$ cells at low frequency (46 cells, 0.12%) (Fig. 3a, Supplementary Fig. 4a). In agreement, real-time PCR analysis showed that expression of the erythropoietic transcription factors *Gata1* [22] and *Klf1* [23] was the highest in 335D1 cells (6.05 times higher than in 212D1 cells and 3.07 times higher than in 256H13 cells) (Fig. 3b). 256H18 and 335D1 cells differentiated into CD45$^+$ leukocytes at 1.32% (4880 cells) and 1.17% (3229 cells), respectively (Fig. 3c, Supplementary Fig. 4b).

Flow cytometry analysis showed that 256H18 cells differentiated into Mac1$^+$/F4/80$^+$ macrophages at high frequency (3622 cells, 0.98%) (Fig. 3d, left panel; Supplementary Fig. 4c, left panel), whereas 335D1 cells differentiated into Gr-1$^+$/F4/80$^-$ granulocytes at high frequency (6738 cells, 2.45%) (Fig. 3d, right panel; Supplementary Fig. 4c, right panel). By contrast, 212B2 cells, which are transduced with the *c-Myc* gene, differentiated into CD45$^+$ leukocytes, Mac1$^+$/F4/80$^+$ macrophages and Gr-1$^+$/F4/80$^-$ granulocytes at low frequency (523, 20 and 756 cells, respectively) (Fig. 3c, d). When we analyzed expression of the leukocyte marker *CD45*, *Csf1r* (encoding colony stimulating factor 1 receptor, a macrophage marker), and *PU.1* (also known as *Spi-1*, which marks the myeloid lineage) at culture day 9, no significant differences were observed among the five lines (Fig. 3e). Taken together, among the five iPSC lines tested, only 256H18 and 335D1 were capable of differentiating at high frequency into both erythroid cells and leukocytes at day 9 of culture.

Expression of Reprogramming and Pluripotency Genes During EB Formation from iPSCs

We next investigated whether pluripotency of iPSCs was related to the nature reprogramming factors used transduce somatic cells. Prior to initiating EB culture, *c-Myc* expression was highest in 212B2 cells, which had been transduced with *c-Myc* along with *Oct3/4*, *Klf4* and *Sox2* genes (Fig. 4a). *Oct3/4* gene expression was highest in 256H13 cells, whereas *Klf4*, *Sox2* and *Nanog* gene expression did not significantly differ among the lines prior to culture. *Oct3/4*, *Klf4* and *Sox2* expression at day 4 of culture was the highest in 212B2 cells, suggesting that they retain pluripotency longer than do the other lines (Fig. 4b).

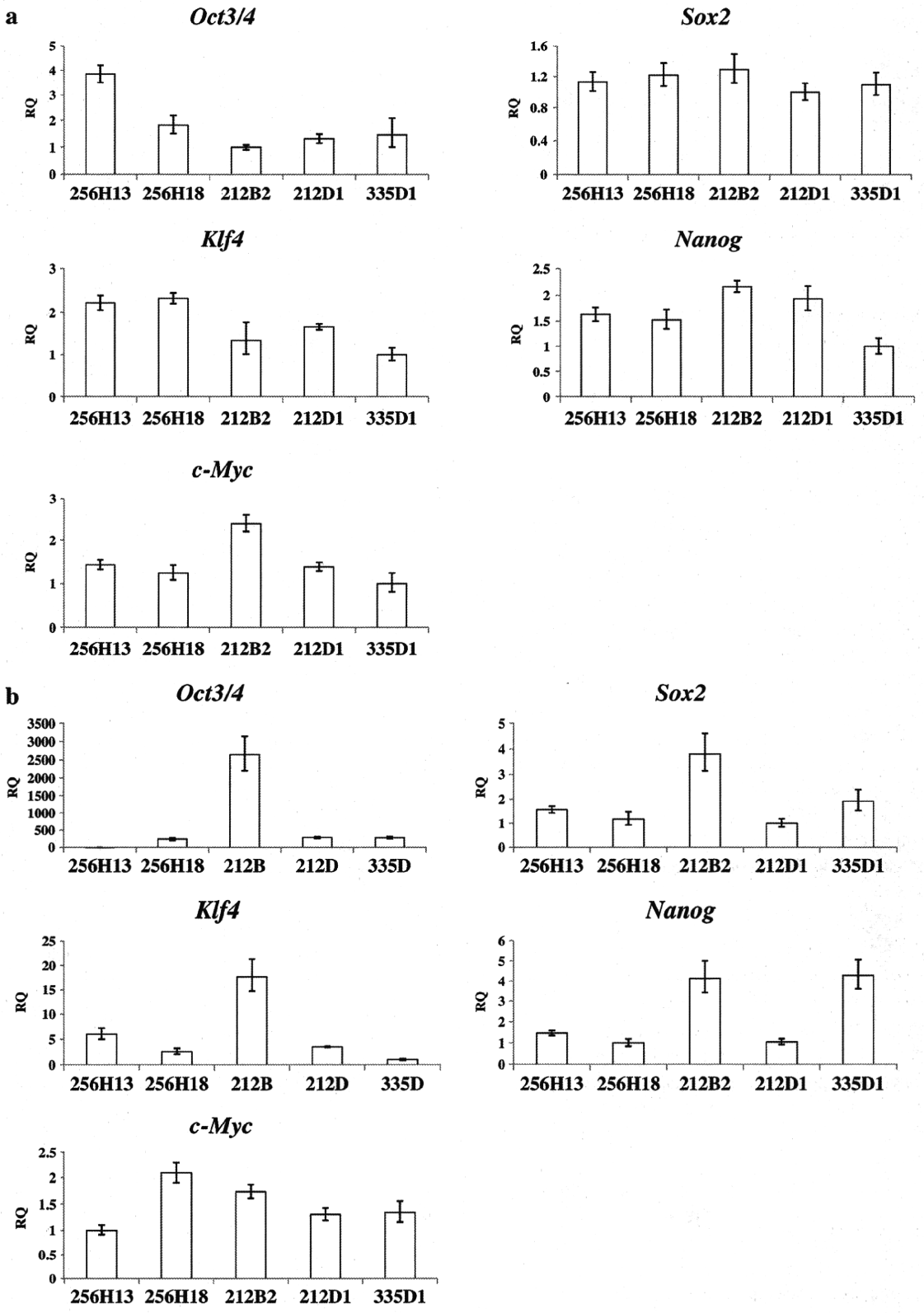

Fig. 4 Comparison of reprogramming and pluripotency gene expression. Quantitative real-time PCR analysis was used to detect expression of the reprogramming genes *Oct3/4, Klf4, Sox2* and *c-Myc* and the pluripotency gene *Nanog* at days 0 (**a**) and 4 (**b**) of EB culture. Data was normalized to *β-actin* expression

Discussion

iPSCs constitute important tools for future regenerative medicine. In this study we compared mesodermal and hematopoietic potential of several iPSC lines, since differentiation potential reportedly varies among iPSC lines established by different sources and methods [12]. Although all iPSCs possessed pluripotency, as defined by expression of *Oct3/4* and *Nanog*, each line showed variations in EB formation and cell proliferation. Examination of mesodermal potential using both flow cytometry and real-time PCR methods, confirmed these differences: specifically, the 256H18 iPSC line gave rise to mesodermal cells at high frequency, whereas 212B2 cells showed the lowest frequency. To identify factors underlying mesodermal potential, we compared expression of both differentiation and pluripotency markers. As summarized in Supplementary Fig. 5, expression of the differentiation markers *Flk1*, *Tbx6*, and *Brachyury* in 256H18 iPSCs was highest at day 4 of culture. Although there was no significant correlation between mesodermal potential and expression of pluripotency markers (Fig. 4), the number of EBs is likely positively correlated with mesodermal potential (Fig. 1). In terms of hematopoietic potential, variations in differentiation capacity were confirmed by flow cytometric and real-time PCR analyses. 256H18 and 335D1 iPSCs generated erythroid cells and leukocytes at high frequency, whereas a low frequency was seen with 212B2 cells (Fig. 3). Expression of the *Oct3/4*, *Sox2*, *Klf4* and *Nanog* pluripotency genes in 256H18 was lowest, whereas 212B2 iPSCs showed highest expression of *Oct3/4*, *Sox2* and *Klf4*. Given the results of our hematopoietic cell differentiation assays at day 4 of culture, these results suggest an inverse relationship between hematopoietic potential and pluripotency gene expression (Fig. 4). *c-Myc* expression in 212B2 cells was highest before culture (Fig. 4a), likely due to ectopic transduction of *c-Myc*. There was a correlation between high *c-Myc* expression and low induction of mesodermal and hematopoietic cells. In our culture conditions, *c-Myc* likely down-regulates mesodermal and hematopoietic cell induction from the 212B2 iPSC line. Our results are compatible with previous reports mentioning that *c-Myc* maintains pluripotency of ESCs [24] and iPSCs [25], and similar to the report showing that c-Myc down-regulates cardiogenic [26] and endodermal differentiation [25] of iPSCs. Taken together, our results imply that iPSCs lacking *c-Myc* transduction will be preferably used for clinical purposes.

Passage number of iPSCs reportedly affected the hematopoietic differentiation [27]. As passage number of iPSCs increased, the transient epigenetic memory of their original somatic cells was gradually lost and hematopoietic differentiation capacity was up-regulated in TTF-derived iPSCs [27]. 256H18 and 335D1 iPSCs generated hematopoietic cells at high frequency, whereas a low frequency was seen in 212B2 in our culture condition (Fig. 3). Since we used iPSC lines of 256H18, 335D1 and 212B2 with similar passage number (P.8- P.10), it is unlikely that passage number affected the hematopoietic differentiation capacity among these three lines. Concerning the other 2 iPSC lines, passage number was lower in 256H13 (P.6-P.9) and 212D1 (P.6) than in 256H18, 335D1 and 212B2. Less hematopoietic cell differentiation in 256H13 and 212D1 than 256H18 and 335D1 was might be due to the difference of passage number.

Taken together, even derived from the same TTF origin, each iPSC demonstrated different mesodermal and hematopoietic potential. Transduction method with retroviral infection and transfection efficiency (20–30%) were similar, while *c-Myc* gene transduction, drug selection with puromycin, reporter genes (Actb-DsRed or Nanog-GFP) and passage number were not identical among five iPSC lines. Therefore, variation in mesodermal and hematopoietic potential was likely affected by combination of transduced genes and passage number, but not transfection methods, drug selection and reporter genes.

Recently, it was reported that iPSCs can be established from peripheral blood (PB) cells [28]. Since collecting a PB sample from a patient is practically easier than taking skin fibroblasts by biopsy in terms of risk and pain, it will be further necessary to evaluate the hematopoietic potential of PB-derived iPSCs in both mice and humans.

Acknowledgements This work was supported by a grant from the Project for Realization of Regenerative Medicine from the Ministry of Education, Culture, Sports, Science and Technology and by a grant from the BASIS project from the Ministry of Education, Culture, Sports, Science and Technology. T. Inoue and K. Kulkeaw is supported by research fellowships from the Ministry of Education, Culture, Sports, Science and Technology, and from The Tokyo Biochemical Research Foundation, respectively. We thank Dr. Keisuke Okita, Ms. Yuka Horio, Ms. Chiyo Mizuochi and the Research Support Center, Graduate School of Medical Sciences, Kyushu University for technical supports, and Dr. Minetaro Ogawa and Dr. Hiroshi Sakamoto for providing LIF. All iPSCs were kindly provided by Dr. Shinya Yamanaka.

Author Contributions Tomoko Inoue performed the experiments, analyzed data and wrote the manuscript. Kasem Kulkeaw, Satoko Okayama and Kenzaburo Tani performed the experiments. Daisuke Sugiyama designed the experiments and wrote the manuscript.

Conflict of Interest All disclosures will be published when the manuscript is accepted.

References

1. Takahashi, K., & Yamanaka, S. (2006). Induction of pluripotent stem cells from mouse embryonic and adult fibroblast cultures by defined factors. *Cell, 126*, 663–676.
2. Wernig, M., Meissner, A., Foreman, R., et al. (2007). In vitro reprogramming of fibroblasts into a pluripotent ES-cell-like state. *Nature, 448*, 318–324.

3. Okita, K., Ichisaka, T., & Yamanaka, S. (2007). Generation of germline-competent induced pluripotent stem cells. *Nature, 448*, 313–317.
4. Yu, J., Vodyanik, M. A., Smuga-Otto, K., et al. (2007). Induced pluripotent stem cell lines derived from human somatic cells. *Science, 318*, 1917–1920.
5. Nelson, T. J., Martinez-Fernandez, A., Yamada, S., Mael, A. A., Terzic, A., & Ikeda, Y. (2009). Induced pluripotent reprogramming from promiscuous human stemness related factors. *Clinical and Translational Science, 2*, 118–126.
6. Nakagawa, M., Koyanagi, M., Tanabe, K., et al. (2008). Generation of induced pluripotent stem cells without Myc from mouse and human fibroblasts. *Nature Biotechnology, 26*, 101–106.
7. Stadtfeld, M., Brennand, K., & Hochedlinger, K. (2008). Reprogramming of pancreatic beta cells into induced pluripotent stem cells. *Current Biology, 18*, 890–894.
8. Okita, K., Nakagawa, M., Hyenjong, H., Ichisaka, T., & Yamanaka, S. (2008). Generation of mouse induced pluripotent stem cells without viral vectors. *Science, 322*, 949–953.
9. Aoi, T., Yae, K., Nakagawa, M., et al. (2008). Generation of pluripotent stem cells from adult mouse liver and stomach cells. *Science, 321*, 699–702.
10. Hanna, J., Markoulaki, S., Schorderet, P., et al. (2008). Direct reprogramming of terminally differentiated mature B lymphocytes to pluripotency. *Cell, 133*, 250–264.
11. Takenaka, C., Nishishita, N., Takada, N., Jakt, L. M., & Kawamata, S. (2010). Effective generation of iPS cells from CD34+ cord blood cells by inhibition of p53. *Experimental Hematology, 38*, 154–162.
12. Kulkeaw, K., Horio, Y., Mizuochi, C., Ogawa, M., & Sugiyama, D. (2010). Variation in hematopoietic potential of induced pluripotent stem cell lines. *Stem Cell Reviews, 6*, 381–389.
13. Huber, T. L., Kouskoff, V., Fehling, H. J., Palis, J., & Keller, G. (2004). Haemangioblast commitment is initiated in the primitive streak of the mouse embryo. *Nature, 432*, 625–630.
14. Lengerke, C., Grauer, M., Niebuhr, N. I., et al. (2009). Hematopoietic development from human induced pluripotent stem cells. *Annals of the New York Academy of Sciences, 1176*, 219–227.
15. Era, T., Izumi, N., Hayashi, M., Tada, S., & Nishikawa, S. (2008). Multiple mesoderm subsets give rise to endothelial cells, whereas hematopoietic cells are differentiated only from a restricted subset in embryonic stem cell differentiation culture. *Stem Cells, 26*, 401–411.
16. Kataoka, H., Takakura, N., Nishikawa, S., et al. (1997). Expressions of PDGF receptor alpha, c-Kit and Flk1 genes clustering in mouse chromosome 5 define distinct subsets of nascent mesodermal cells. *Development, Growth & Differentiation, 39*, 729–740.
17. Sakurai, H., Era, T., Jakt, L. M., Okada, M., Nakai, S., & Nishikawa, S. (2006). In vitro modeling of paraxial and lateral mesoderm differentiation reveals early reversibility. *Stem Cells, 24*, 575–586.
18. Choi, K., Kennedy, M., Kazarov, A., Papadimitriou, J. C., & Keller, G. (1998). A common precursor for hematopoietic and endothelial cells. *Development, 125*, 725–732.
19. Fehling, H. J., Lacaud, G., Kubo, A., et al. (2003). Tracking mesoderm induction and its specification to the hemangioblast during embryonic stem cell differentiation. *Development, 130*, 4217–4227.
20. Chapman, D. L., Agulnik, I., Hancock, S., Silver, L. M., & Papaioannou, V. E. (1996). Tbx6, a mouse T-Box gene implicated in paraxial mesoderm formation at gastrulation. *Developmental Biology, 180*, 534–542.
21. Wilkinson, D. G., Bhatt, S., & Herrmann, B. G. (1990). Expression pattern of the mouse T gene and its role in mesoderm formation. *Nature, 343*, 657–659.
22. Whitelaw, E., Tsai, S. F., Hogben, P., & Orkin, S. H. (1990). Regulated expression of globin chains and the erythroid transcription factor GATA-1 during erythropoiesis in the developing mouse. *Molecular and Cellular Biology, 10*, 6596–6606.
23. Miller, I. J., & Bieker, J. J. (1993). A novel, erythroid cell-specific murine transcription factor that binds to the CACCC element and is related to the Kruppel family of nuclear proteins. *Molecular and Cellular Biology, 13*, 2776–2786.
24. Varlakhanova, N. V., Cotterman, R. F., & deVries, W. N. (2010). Myc maintains embryonic stem cell pluripotency and self-renewal. *Differentiation, 80*, 9–19.
25. Smith, K. N., Singh, A. M., & Dalton, S. (2010). Myc represses primitive endoderm differentiation in pluripotent stem cells. *Cell Stem Cell, 7*, 343–54.
26. Martinez-Fernandez, A., Nelson, T. J., Ikeda, Y., & Terzic, A. (2010). c-MYC independent nuclear reprogramming favors cardiogenic potential of induced pluripotent stem cells. *Journal of Cardiovascular Translational Research, 3*, 13–23.
27. Polo, J. M., Liu, S., & Figueroa, M. E. (2010). Cell type of origin influences the molecular and functional properties of mouse induced pluripotent stem cells. *Nature Biotechnology, 28*, 848–55.
28. Loh, Y. H., Agarwal, S., & Park, I. H. (2009). Generation of induced pluripotent stem cells from human blood. *Blood, 113*, 5476–9.

Genes to Cells

Cold exposure down-regulates zebrafish pigmentation

Kasem Kulkeaw[1], Tohru Ishitani[2], Takaaki Kanemaru[3], Ognen Ivanovski[1,4], Midori Nakagawa[1], Chiyo Mizuochi[1], Yuka Horio[1] and Daisuke Sugiyama[1]*

[1]*Department of Hematopoietic Stem Cells, SSP Stem Cell Unit, Faculty of Medical Sciences, Kyushu University, Fukuoka, Japan*
[2]*Division of Cell Regulation Systems, Department of Post-Genome Science Center, Medical Institute of Bioregulation, Kyushu University, Fukuoka, Japan*
[3]*Morphology Core Unit, Kyushu University Hospital, Fukuoka, Japan*
[4]*University Clinic of Urology, Medical Faculty, University 'Ss Cyril and Methodius,' Skopje, Macedonia*

Vertebrates use adaptive mechanisms when exposed to physiologic stresses. However, the mechanisms of pigmentation regulation in response to physiologic stresses largely remain unclear. To address this issue, we developed a novel pigmentation model in adult zebrafish using coldwater exposure (cold zebrafish). When zebrafish were maintained at 17 °C, the pigmentation of their pigment stripes was reduced compared with zebrafish at 26.5 °C (normal zebrafish). In cold zebrafish, gene expression levels of *tyrosinase* and *dopachrome tautomerase*, which encode enzymes involved in melanogenesis, were down-regulated, suggesting that either down-regulation of melanin synthesis occurred or the number of melanophores decreased. Both regular and electron microscopic observation of zebrafish skin showed that the number of melanophores decreased, whereas aggregation of melanosomes was not changed in cold zebrafish compared with normal zebrafish. Taken together, we here show that cold exposure down-regulated adult zebrafish pigmentation through decreasing the number of melanophores and propose that the cold zebrafish model is a powerful tool for pigmentation research.

Introduction

Cold temperatures affect many physiologic processes in endothermic animals, such as slowing the rate of enzymatic reactions, reducing diffusion and transport of biologic molecules, inducing protein denaturation and misaggregation, slowing gene transcription and translation, disrupting cytoskeletal structure and altering cell membrane permeability (Sonna *et al.* 2002). In contrast to endothermic animals, ectothermic vertebrates, such as fish, possess multiple adaptation mechanisms that allow them to cope with low temperatures, which are as follows: (i) increasing the quantity of enzymes involved in lipid metabolism (Cossins *et al.* 2002), (ii) increasing pump activity, Na^+/K^+-ATPase activity and oxygen consumption in hepatocytes and kidney cells (Schwarzbaum *et al.* 1992a,b) and (iii) up-regulation of genes related to oxidative stress in the skeletal muscle of fish tails (Malek *et al.* 2004). Environmental temperature has been shown to affect the expression levels of the cold-shock proteins (Al-Fageeh & Smales 2006). Low temperature (17 °C) induces the expression of cold-shock domain (CSD) containing C2 (*csdc2*) gene in zebrafish kidney marrow (KM) (Kulkeaw *et al.* 2010). Csdc2 contains an S1-like CSD, which is widely found in the cold-shock proteins of eukaryotes, prokaryotes and archaea. Although the functions of cold-shock proteins remain unclear, they have been shown to bind mRNA to regulate ribosomal translation, mRNA degradation and rate of transcription termination (Al-Fageeh & Smales 2006). Heat-shock proteins are also related to environmental temperature, and expression of *heat shock protein 8* (*hspa8*) decreases in carp when exposed to coldwater temperature (Ali *et al.* 2003).

Studies of zebrafish (*Danio rerio*), a teleost tropical fish, have enhanced our understanding of human and mouse developmental biology. Easy handling of embryos and a short lifespan make zebrafish a suitable

Communicated by: Shigeru Kondo
**Correspondence*: ds-mons@yb3.so-net.ne.jp

DOI: 10.1111/j.1365-2443.2011.01498.x

model for investigations into cellular differentiation, organ development and gene function via genetic manipulation. Zebrafish have also been used in pigmentation research. For example, studies of pigment cell differentiation during zebrafish development have produced several mutant strains: *albino*^{b1}, *golden*^{b2}, *brass*^{b4}, *sparse*^{b5} (Parichy *et al.* 1999), *leopard*^{t1} (Johnson & Weston 1995) and *panther*^{j4blue} (Parichy *et al.* 2000). These studies show that zebrafish is a useful genetic model for studying developmental biology in the field of pigmentation research. In adult zebrafish, pigment is represented as blue and black stripes running along the body length and fins, separated by silver interstripes. The pigment cells (chromatophores) are localized in the hypodermis. Zebrafish have three types of chromatophores: xanthophores (yellow), reflective iridophores and melanophores (black), in order from superficial to deep. Pigmented melanophore formation in adult zebrafish requires the differentiation from melanoblasts, melanin synthesis and translocation of melanin-containing granules, or melanosomes. Melanoblast differentiation has been extensively studied in fin regeneration, and *kita* and *kit ligand a* (*kitlga*) have been identified as crucial proponents (Rawls & Johnson 2000, 2001). *Microphthalmia-associated transcription factor a* (*mitfa*) also plays an important role, by controlling the expression of genes encoding the melanin-synthesizing enzymes, *tyrosinase* (*tyr*) and *dopachrome tautomerase* (*dct*) (White & Zon 2008). It appears that *mitfa* is an early marker of melanoblast differentiation (Lister *et al.* 1999), followed by *kita* (Parichy *et al.* 1999) and *dct* (Kelsh & Eisen 2000). Nonpigmented melanophore then synthesizes melanin, which is stored in melanosomes. The melanosomes are then distributed throughout the cytoplasm of melanophore. It has been reported that melanin-concentrating and melanocyte-stimulating hormones (MCH and MSH, respectively) control melanosome translocation (Logan *et al.* 2006). Both hormones are synthesized in brain and have antagonist effects. MCH is derived from pro-melanin-concentrating hormone (*pmch*) and causes melanosome aggregation, whereas MSH is derived from proopiomelanocortin a (*pomca*) and causes melanosome dispersion. In addition to hormone, aggregation of melanosome of fish melanophores is controlled by sympathetic neurons (Iwashita *et al.* 2006). However, the mechanisms of pigmentation regulation in response to physiologic and environmental stresses remained ill-defined. Alternative pigmentation models are necessary to address this issue. In response, we here show a novel model in zebrafish using coldwater exposure.

Results

Cold exposure down-regulates skin pigmentation in zebrafish

No significant differences were observed between the two groups of zebrafish before cold exposure (results not shown). On day 3 of exposure of one group to cold water, pigmentation of cold zebrafish (17 °C) began to become slightly paler than that of normal zebrafish (26.5 °C) (Fig. 1A). One week after cold exposure, the pigmentation of the cold zebrafish,

Figure 1 Effects of cold exposure on zebrafish pigmentation and growth. (A) Gross appearances of normal and cold zebrafish and their background adaptation. Normal and cold zebrafish were maintained at 26.5 or 17 °C inside of incubator for 3 days (d), 1 week (W) and 2 W. The cold zebrafish appeared pale and depigmented. The degree of depigmentation correlated with the length of cold exposure. In background adaptation (lower panel), zebrafish were maintained at 26.5 °C in the incubator with appropriate light cycle. Two weeks later, the pigmentation of control zebrafish inside of incubator became slightly pale compared with zebrafish maintaining in water tank. (B) Higher magnification of pigment stripes on the body and tail. At 2 W, melanophores of cold zebrafish appeared as spots, whereas melanophores of normal zebrafish spread over larger areas. (C) Melanin content in zebrafish skin. The zebrafish skin was solubilized in Soluene®-350. Melanin was measured by absorption at 500 nm. The bar graphs show the means and standard deviation of optical density per 50 mg of zebrafish skin from three zebrafish per group. The Student's *t*-test was used for statistical analysis. (D) Effects of cold exposure on body weight and size of zebrafish. Cold exposure reduced the growth of zebrafish. Two-month-old zebrafish were maintained in water at 26.5 or 17 °C for 1 W, 2 W and 7 months (Mo). Body weight and length of cold zebrafish were significantly lower than those of normal zebrafish (upper and lower panels, respectively). The bar graphs show the means and standard deviations of body weight and length from 6 to 7 zebrafish per group. Student's *t*-test was used for statistical analysis. (E) Histology of kidney marrow (KM). KM was stained with Toluidine Blue O (left and middle) and observed by transmission electron microscopy (TEM) (right). In 26.5 °C water, there are normal renal tubules (RT) surrounded by hematopoietic cells (HC) (left). Cold zebrafish kept at 17 °C for 7 Mo exhibit abnormal RTs (upper middle). Black pigment-producing cells (lower middle, arrow) were observed only in cold zebrafish. TEM image shows melanin-containing granules in the KM of cold zebrafish (right).